Quaternary Science Reviews 179 (2018) 158–166

Contents lists available at ScienceDirect

Quaternary Science Reviews

journal homepage: www.elsevier.com/locate/quascirev

$\delta^{13}C$ signal of earthworm calcite granules: A new proxy for palaeoprecipitation reconstructions during the Last Glacial in western Europe

Charlotte Prud'homme [a, b, f, *], Christophe Lécuyer [b, 1], Pierre Antoine [a], Christine Hatté [c], Olivier Moine [a], François Fourel [b], Romain Amiot [b], François Martineau [b], Denis-Didier Rousseau [d, e]

[a] Laboratoire de Géographie Physique, Environnements Quaternaires et Actuels, (LGP), UMR 8591 CNRS-Université Paris 1-UPEC, 1 place Aristide Briand, 92195 Meudon Cedex, France
[b] Laboratoire de Géologie de Lyon (LGL–TPE), UMR CNRS 5276, Université Claude Bernard Lyon 1, 2 Rue Raphaël Dubois, 69622 Villeurbanne Cedex, France
[c] Laboratoire des Sciences du Climat et de l'Environnement, UMR CEA-CNRS-UVSQ 8212, Université Paris Saclay, 91198 Gif-sur-Yvette Cedex, France
[d] Laboratoire de Météorologie Dynamique, UMR CNRS 6539, PSL Research University, CERES-ERTI, 24 Rue Lhomond, 75231 Paris, France
[e] Lamont-Doherty Earth Observatory of Columbia University, Palisades, NY 10964, USA
[f] Research Group for Terrestrial Palaeoclimates, Max Planck Institute for Chemistry, Hahn-Meitner-Weg 1, 55128 Mainz, Germany

ARTICLE INFO

Article history:
Received 23 June 2017
Received in revised form
28 September 2017
Accepted 13 November 2017

Keywords:
Earthworm calcite granules
Carbon stable isotopes
Palaeoprecipitation reconstructions
Loess-palaeosol sequence
Nussloch

ABSTRACT

Quantification of paleoprecipitation during the Last Glacial is a key element to reconstruct palaeoclimates. Recently, fossil calcite granules have been identified in loess sequences with high contents in specific horizons. In this study, we explored for the first time the potential of this new bio-indicator as a climatic proxy for precipitation in western Europe during the Last Glacial. We extracted 30 granules from eleven samples belonging to three tundra gleys and two brown soils from the Nussloch loess sequence previously dated between 50 and 20 ka. Stable carbon isotope measurements were performed on each granule and duplicated. Throughout the studied section, $\delta^{13}C$ values range from −15.4 to −10.3‰ for tundra gleys and from −14.9 to −9.5‰ for brown soils. By taking into account the fractionation factor between the carbon ingested by the earthworm and the carbon output of the granules, the $\delta^{13}C$ values of these granules reflect the composition of the C_3 plant vegetation cover. Thus, we estimated the $\delta^{13}C$ of the plants with a mean value of -24.3 ± 0.9‰ for tundra gleys and -24.1 ± 0.9‰ for brown soils, which are in agreement with values obtained from organic matter preserved in sediments. Palaeoprecipitation range over both tundra gley horizons and brown soils were estimated at about 333[159–574] mm/yr by using an empirical relationship determined between present-day plant leaf isotopic discrimination and the mean annual precipitation. This original preliminary study highlights the potential of earthworm calcite granule $\delta^{13}C$ measurements as a new proxy for paleoprecipitation during the Last Glacial interstadials in continental environments.

1. Introduction

The Last Glacial (from 110 to 15 ka) is certainly the most intensively studied period for understanding the past climate dynamics. This period is characterized by rapid climate variations highlighted in the Greenland ice core records (Dansgaard et al., 1993; NGRIP members, 2004; Rasmussen et al., 2014) and in marine sediments (Heinrich, 1988; Bond et al., 1992; Sánchez Goñi et al., 2008). These millennial climate variations are also recorded in terrestrial archives in Europe such as lacustrine sedimentary deposits, pollen records, speleothems and loess-palaeosol sequences (Antoine et al., 2009; Genty et al., 2010; Harrison and Goñi, 2010; Moreno et al., 2014). Understanding the palaeoclimate of the Last Glacial is important to correctly set up and test the numerical models designed to simulate the forthcoming Earth's climates. So

* Corresponding author. Research Group for Terrestrial Palaeoclimates, Max Planck Institute for Chemistry, Hahn-Meitner-Weg 1, 55128 Mainz, Germany.
E-mail address: c.prudhomme@mpic.de (C. Prud'homme).
[1] Also at Institut Universitaire de France.

https://doi.org/10.1016/j.quascirev.2017.11.017
0277-3791/

far, most of the palaeoclimate studies mainly focused on temperature reconstructions (Rousseau, 1991; Rousseau et al., 2002, 2007; Ampel et al., 2010; Moreno et al., 2014; Prud'homme et al., 2016). However, the quantification of the amount of precipitation during the Last Glacial is a key element to evaluate the potential resources that were available for the biomass development and hydrological cycle. It is worthy to note that Zech et al. (2013) attempted to estimate amounts of paleoprecipitation on the basis of biomarkers.

In this context, the European loess belt represents the most extended sedimentary archive of the Last Glacial. The loess-palaeosol sequences from this area are characterized by high sedimentation rates especially between ~30 ka and 17 ka, and are punctuated by palaeosol horizons (boreal to arctic brown soils, and tundra gley horizons) testifying a milder climate (interstadials) of various intensity and duration (Moine et al., 2017; Rousseau et al., 2017). These archives therefore constitute valuable records to depict the abrupt climate changes that impacted the terrestrial environments during the Last Glacial. Moreover, loess sequences have been dated through the use of different absolute geochronological methods (OSL and ^{14}C) (Bibus et al., 2007; Rousseau et al., 2007; Tissoux et al., 2010; Moine et al., 2017). This precise chronology led to refine correlations between the various pedogenic horizons occurring in western European loess records and the Dansgaard-Oeschger events from Greenland ice cores (Rousseau et al., 2002, 2007; Moine, 2008; Antoine et al., 2009; Haesaerts et al., 2016; Moine et al., 2017).

In this environment, several types of secondary carbonates have been found including calcified roots (rhizoliths), carbonate coatings, hypocoatings (Becze-Deak et al., 1997; Barta, 2014), from which stable isotope analyses were performed (Gocke et al., 2011; Koeniger et al., 2014). The $\delta^{13}C$ values of pedogenetic or soil carbonates are mainly inherited from the oxidation of soil organic matter through the action of microorganisms. This organic matter partly derives from plants whose $\delta^{13}C$ values are related to the carbon isotope composition of atmospheric carbon dioxide (Cerling and Quade, 1993). In natural environments, the large range of $\delta^{13}C$ values of both soil organic matter and soil carbonate reflects variations in the proportions of C_3, C_4 or Crassulacean Acid Metabolism (CAM) plants (O'Leary, 1981; Cerling and Quade, 1993). Plants absorb the atmospheric CO_2 through distinct metabolic pathways that depend on the climate and the environment where the plants are growing. The most common mode used by plants is the C_3 Calvin Benson cycle, characteristic of mild and humid climates. C_3 plants have low $\delta^{13}C$ values ranging from −34‰ to −22‰ and averaging −27‰ (O'Leary, 1981). The C_4 plants found in tropical and dry environments operate photosynthesis by following the Hatch Slack cycle, a less discriminating pathway relative to ^{13}C, leading to less negative $\delta^{13}C$ values of organic matter (from −18‰ to −8‰) with a mean of −13‰(O'Leary, 1981). The last type of photosynthesis is the Crassulacean Acid Metabolism (CAM). CAM plants are relatively rare (~5%) on Earth and occur in desert-like environments, they fix the carbon from the atmospheric CO_2 either via the ribulose biphosphate carboxylase (C_3 pathway) or via both carboxylation and reduction of phosphoenolpyruvate (C_4-like cycle). Therefore, CAM plants are characterized by a range of $\delta^{13}C$ values mostly spanning those of C_3 and C_4 plants (O'Leary, 1981).

By taking into account the carbon isotope fractionation that takes place during the oxidation of organic matter into carbonate, the $\delta^{13}C$ values of rhizoliths extracted from the Nussloch loess section (Germany) revealed that they derived from C_3 plants (Gocke et al., 2011). This is in agreement with the $\delta^{13}C$ values of the organic matter preserved in this loess section, which also reflect those of a vegetation cover that only consisted of C_3 plants (Hatté et al., 2001; Hatté and Guiot, 2005) as observed in several European sequences although C_4 excursions were noticed pointing to climatic variability (Hatté et al., 2013). Carbon isotope compositions of organic matter preserved in loess sequences have also been used to reconstruct palaeoprecipitation during the Last Glacial interval by using an empirical equation (Hatté et al., 2001) and the model BIOME 4 (Hatté and Guiot, 2005).

Apart from terrestrial molluscs and secondary carbonates, European loess sequences have a very low content in bio-indicators. In this context, a new proxy has been recently studied: the fossil earthworm calcite granules. These granules are well correlated with some specific features of the pedostratigraphy. Indeed, the concentration is high in palaeosols (tundra gley horizons and boreal/arctic brown soils) whereas it is rare to absent in pure typical loess deposits (Prud'homme et al., 2015). In addition, the occurrence of a permanently frozen layer below the tundra gley horizons (typically 0.23–0.5 m thick), implies that earthworms were confined in the upper part of the soil profiles and thus produced granules that are strictly contemporaneous of these former active layer horizons. This assumption is confirmed by the radiocarbon dates from fossil earthworm granules extracted from the Nussloch sequences (Moine et al., 2017). This new proxy has also been proposed as a new palaeothermometer for the warmest season during the interstadials in terrestrial environment (Prud'homme et al., 2016).

We propose here that the $\delta^{13}C$ values of fossil earthworm calcite granules could constitute a proxy of past rainfall. Those estimates of paleoprecipitation can be compared to those inferred from the carbon isotopic composition of organic matter by using the model BIOME 4. Indeed, the $\delta^{13}C$ values of plants ($\delta^{13}C_{pl}$) can be estimated from those of earthworm calcite granules ($\delta^{13}C_{ECG}$) taking into account the isotopic fractionation factor of -11.7 ± 1.5‰ (Canti, 2009) between the diet-derived carbon ingested by the earthworms and the mineralized carbon of the granule made of pure calcite. Granules were extracted from specific horizons (tundra gleys, arctic and boreal brown soils) of the Nussloch loess sequences as they contain high amount of earthworm calcite granules (up to 400–500). Similar to the former P2, P3 and P4 profiles (Antoine et al., 2009, 2001), the 17-m-thick Nussloch P8 profile, also spanning the 55 to 20 ka time interval, is thus considered as one of the most complete records of the Last Glacial in western Europe. In the present study, we explore the potential of earthworm calcite granule $\delta^{13}C$ values as a new proxy for precipitation during the Last Glacial interstadials in continental environments by using an empirical relationship determined between present-day plant leaf isotopic discrimination and the mean annual precipitation.

2. Material and methods

2.1. Stratigraphy of Nussloch loess sequence

Fossil earthworm calcite granules were extracted from the 17 m-thick Nussloch P8 profile. This section is exposed within an active quarry located at 49°18′59″N, 8°43′54″E, about ten kilometers SSE of Heidelberg. The correlation between the stratigraphy and the lithology of the different profiles revealed two main parts (Fig. 3) (Antoine et al., 2001, 2009).

The lower part of the sequence is characterized by the occurrence of three well preserved brown palaeosols: two thick (~1 m) boreal brown soils, the Lower and Upper Gräselberger Boden (GBL and GBU after Schönhals et al. (1964)) and one 0.4-m thick arctic brown soil (Lohner Boden, LB after Semmel (1973)). These three soils developed during the Middle Pleniglacial interstadials from ~55 to ~35 ka (mostly MIS 3) are characterized by the formation of a Bw cambic horizon (Antoine et al., 2001). They are separated by aeolian sands, loess, and two tundra gley horizons, the whole representing a 5-m thick soil complex. The formation of these two cambisols (Gräselberger and Lohner boden) indicated a climatic improvement, a densification of the vegetation and an increased biological activity demonstrated by the analysis of the pedostratigraphy and of the mollusc assemblage (Antoine et al., 2001; Moine et al., 2008). Additionally, the Lohner Boden is marked by a platy microstructure (periglacial feature), hence being and thus, it can be classified as a Gelic cambisol or an arctic brown soil (Tedrow, 1977).

The upper part is characterized by a high sedimentation rate (reaching ~1 mm/yr in average between 30 and 20 ka) that led to a 12-m-thick deposit correlated with the Upper Pleniglacial dated between 35 and 15 ka (end of MIS 3 and MIS 2). This sequence is characterized by a cyclic alternation of typical calcareous loess units and the development of tundra gley horizons.

The occurrence of cryo-injection and former ice-wedges in tundra gley horizons demonstrated that they have been developed in a permafrost environment. These gley horizons are formed by hydromorphic processes resulting from the active layer decay of a former permafrost. The presence of waterlogging is characterized by a reduction of iron and a slight decalcification with redistribution of carbonate at the base of the profile (Antoine et al., 2009; Taylor and Lagroix, 2015).

2.2. Earthworm calcite granules production and sampling strategy

According to observations in the present day environments and in laboratory experiments, calcite granules are produced by earthworms that released them in the first upper centimetres of the soil (Bräm, 1956; Canti, 1998; Canti and Piearce, 2003). They are collected with high abundance (200–500 granules by 10 litres of sediments) in both tundra gleys horizons and boreal and arctic brown soils (Prud'homme et al., 2015). These granules of 0.5–1 mm (Fig. 1) are composed of rhombohedra calcite crystals (Canti, 1998; Gago-Duport et al., 2008) organized in a radial crystalline structure. The biomineralization processes start with the crystallization of amorphous calcium carbonate (ACC) within the calciferous earthworm glands which contain a milky fluid (Lee et al., 2008; Hodson et al., 2015). These glands, located in pairs on each side of the oesophagus in segments 10, 11 and 12 (Fig. 1), are well developed in *Lumbricus* (Darwin, 1881). The milky fluid reaches the oesophageal pouches where the former calcium carbonate precipitate evolves into macroscopic crystals of calcium carbonate, which are finally released into the soil through the gut (Briones et al., 2008; Gago-Duport et al., 2008). The production of a granule is very rapid, as the crystallization of ACC is completed within 24 h (Lee et al., 2008). Among the most common species in United Kingdom, *Lumbricus* is the most important granule-producer genus (Bräm, 1956; Canti and Piearce, 2003).

The new profile P8 from Nussloch was firstly cleaned vertically over 50 cm in order to describe properly the sedimentary sequence. Then, the sequence was sampling at high resolution every 5 cm throughout the 17-m thick outcrop. Each sample had the same volume of 10 litres. Samples of 10 litres of sediment were wet-sieved to remove the sediment fraction under 0.425 mm. Then, earthworm calcite granules larger than 0.8 mm were extracted to mainly focus on those produced by the *Lumbricus* genus (Canti, 1998; Canti and Piearce, 2003).

Earthworm calcite granules were collected from eleven 5-cm-thick samples from 1) Four tundra gley units G7, G2b, G2a and G1 (5 samples numbered from P8-1 to P8-5), 2) from one arctic brown soil, Lohner Boden (3 samples numbered from P8-6 to P8-8) and 3) one boreal brown soil, Gräselberger Boden (3 samples numbered from P8-9 to P8-11) (Fig. 3).

2.3. Stable isotope analysis

We used the same extraction and preparation protocol than that applied to oxygen isotope measurements (Prud'homme et al., 2016). After being cleaned in an ultrasonic bath with deionized water to remove any remaining sediment matrix, thirty granules were selected from each sample for stable isotope analyses. The two main criteria of the final selection of the granules were the absence of impurities and the presence of well-preserved surface crystals (Fig. 1).

Each granule was crushed in an agate mortar until a fine powder (granulometry ≈ 50 μm) was obtained. Stable carbon isotope ratios ($\delta^{13}C_{ECG}$) of those powdered individual granules were measured by using an auto sampler Multiprep™ system coupled to a dual-inlet GV Isoprime™ isotope ratio mass spectrometer (IRMS) at the Laboratoire de Géologie of the University of Lyon. For each granule, two aliquots of about 200–300 μg of calcium carbonate were reacted with oversaturated anhydrous phosphoric acid at 90 °C during 20 min. Isotope compositions are quoted in the delta notation in ‰ relative to V–PDB. Isotopic data result from a two-point calibration using both the international reference NIST NBS18 (−5.00 ± 0.04‰, N = 60) and the internal reference 'Carrara Marble' (2.02 ± 0.03‰, N = 180), itself regularly calibrated against the international reference NIST NBS19. The Table S1 contains all the $\delta^{13}C$ values (N = 330) of earthworm granules along with the standard deviations. Each granule was replicated to obtain better precision. External reproducibility is ±0.05‰ for $\delta^{13}C$ values (2σ). In total, we measured 330 granules corresponding to 660 aliquots of calcite.

3. Results

3.1. Carbon isotope compositions of earthworm calcite granules

Carbon isotope compositions of earthworm granules obtained from the eleven layers of Nussloch profile P8 are compiled in Table 1 along with mean values and standard deviations (SD). Among the 330 analyzed earthworm calcite granules (Table S1), the carbon isotope ratios range from −15.4‰ to −9.5‰ (V-PDB) with a mean value of −12.5 ± 0.9‰ (Table 1). First of all, the Shapiro-Wilk test was used to check if the $\delta^{13}C$ values follow a normal distribution. The tests for the overall results (n = 330) and the tundra gley values (n = 150) do not reject the null hypothesis (p-value = 0.192 and 0.128). The p-value for the brown soils is closed to 0.05 (p = 0.045), thus, we can assume that the values are normally distributed.

The mean granule $\delta^{13}C$ values from tundra gleys are −12.6 ± 0.9‰ and brown soils −12.4 ± 0.9‰, respectively (Fig. 2). We used the t–student test to check whether or not the mean values of two populations are statistically different at a significance threshold of 95%. A p-value higher than 0.05 validates the null hypothesis. Indeed, t–tests indicate that the granule $\delta^{13}C$ values are not statistically different (p-value = 0.187) between the tundra gley horizons, and boreal and arctic brown soils.

3.2. Processing raw data

3.2.1. $\delta^{13}C$ of plants inferred from the $\delta^{13}C$ of earthworm calcite granules

It is important to identify the source of carbon in the granules before any attempt to reconstruct palaeoprecipitation. Canti (2009) performed several experiments to track the potential sources of carbon constituting the *Lumbricus terrestris* calcite granules. The artificial soils were composed of material with variable $\delta^{13}C$ values (litter, the soil organic matter and the soil calcium carbonate), while the $\delta^{13}C$ of ambient atmospheric carbon dioxide was fixed to −8‰.

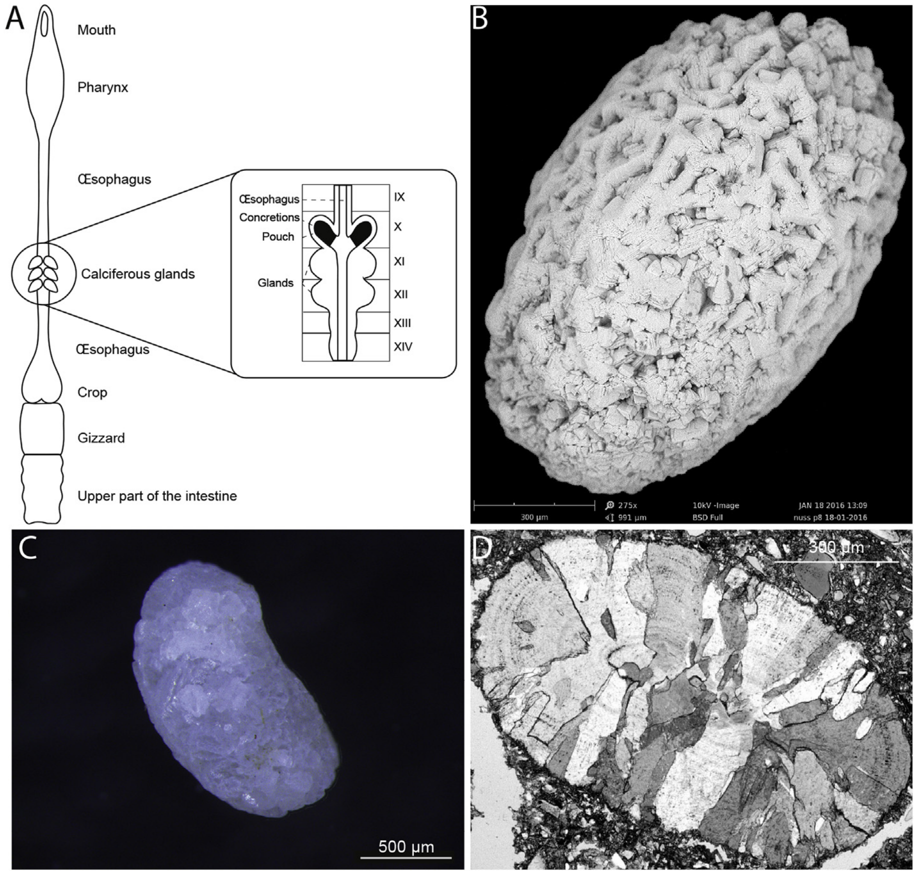

Fig. 1. A) Schema of the calciferous glands of *Lumbricus terrestris* from (Canti, 1998; Darwin, 1881), B) Scanning Electron Microscopy of an earthworm calcite granule from the Nussloch P8 loess profile (SEM), C) Photomicrograph of one earthworm calcite granule extracted from a tundra gley horizon, Nussloch P8, D) Thin section of an earthworm calcite granule from Villiers-Adam Middle Pleniglacial brown soils (photo P. Antoine).

The results showed that the main source of carbon in the calcite granule is coming from a mixture of litter and soil organic matter (earthworm diet), even though atmospheric carbon may contribute to the total budget of mineralized carbon stored in the granule, especially for the epigeic species, i.e earthworm species living near the soil surface (Canti, 2009; Canti et al., 2015). The result of the experiments conducted by Canti (2009) implied that a carbon isotope fractionation of −11.7 ± 1.5‰ takes place between the carbon ingested by the earthworms and the carbon integrated in the granules. This value includes the carbon isotope fractionation between amorphous calcium carbonate (ACC) and calcite produced by earthworm ($\varepsilon_{\text{calcite-ACC}} = -1.2 \pm 0.5‰$) measured by Versteegh et al. (2017). We assumed that this isotopic fractionation was constant through time. Consequently, the mean $\delta^{13}C$ value of the vegetation can be estimated from the carbon isotope composition of the calcite granules: −24.3 ± 0.8‰ for tundra gley horizons and −24.1 ± 0.9‰ for brown soils. The calculated mean $\delta^{13}C_{pl}$ values for the different horizons are in agreement with a main source of organic matter derived from C_3 plants as already proposed by Hatté et al. (2001).

Table 1
Mean and standard deviations of $\delta^{13}C$ values (‰ V-PDB) of earthworm calcite granules recovered from four tundra gley horizons (G1, G2, G4 and G7), from an arctic brown soil (Lohner Boden (LB)) and a boreal brown soil (Gräselberger Boden Upper (GBU)) of the Nussloch loess sequence (P8), Germany. Samples are located along the stratigraphic sequence (cm) of Fig. 3 and « n » represents the number of analyzed samples.

Level (cm)	Sample	Horizon	n	Mean $\delta^{13}C$ (‰V-PDB)
295–300	P8_1	G7	30	−12.0 ± 0.7
1025–1030	P8_2	G2a	30	−12.6 ± 0.9
1055–1060	P8_3	G2b	30	−12.7 ± 0.9
1105–1110	P8_4	G2d	30	−13.2 ± 0.9
1175–1180	P8_5	G1	30	−12.4 ± 0.8
1200–1205	P8_6	LB	30	−12.7 ± 0.6
1210–1215	P8_7	LB	30	−12.6 ± 0.9
1220–1225	P8_8	LB	30	−12.5 ± 0.9
1395–1400	P8_9	GBU	30	−12.2 ± 0.8
1405–1410	P8_10	GBU	30	−12.5 ± 0.8
1415–1420	P8_11	GBU	30	−12.2 ± 1.2

3.2.2. *Palaeoprecipitation reconstructions*

We used an empirical method to reconstruct the palaeoprecipitation. This method is based on a relationship determined between plant leaf discrimination ($\Delta^{13}C_{pl}$) and the mean annual precipitation (MAP) (Kohn, 2010). The dataset of Kohn (2010) is a compilation of modern carbon isotope compositions of all types of C_3 plants sampled from 480 sites, which are associated with the mean annual precipitation. Rey et al. (2013) computed a new linear regression between $\Delta^{13}C_{leaf}$ and$\log_{10}$(MAP+300) based on the dataset provided by Kohn (2010). Even if the study of Kohn (2010) is under debate (Diefendorf et al., 2010; Freeman et al., 2011; Kohn, 2011), this empirical method provides a first approximation to estimate palaeoprecipitation from the $\delta^{13}C$ values of the granules. Moreover, our estimates can be compared to the results given by Hatté and Guiot (2005), which were based on a model simulation (BIOME 4) from the $\delta^{13}C$ of the organic matter in Nussloch.

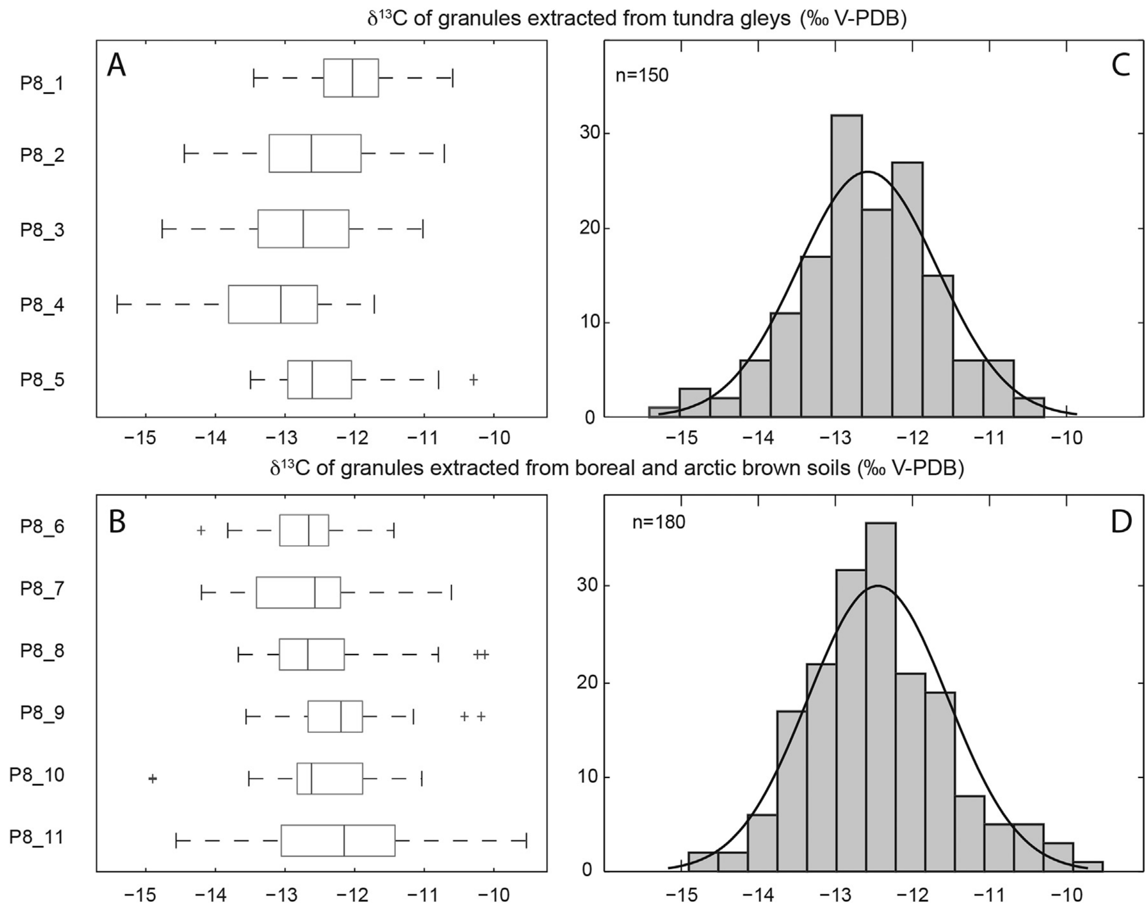

Fig. 2. Boxplots and frequency histograms illustrating the carbon isotope compositions of earthworm calcite granules from tundra gley horizons and brown soils from Nussloch loess sequences. A) Granules were extracted from four tundra gley horizons (G1, G2a, G2b, G7; samples from P8-1 to P8-5) and B) from an arctic brown soil (Lohner Boden, samples from P8-6 to P8-8) and a boreal brown soil (Upper Gräselberger Boden, samples from P8-9 to P8-11). Each boxplot represents the results of 30 granules. C) Frequency histograms for tundra gley horizons and D) for arctic and boreal brown soils.

$$Log_{10}\left(MAP + 300\left(mm.yr^{-1}\right)\right) = 0.092(\pm 0.004)\Delta^{13}C_{pl} + 1.148(\pm 0.074) \quad (1)$$

($R^2 = 0.56$; $\sigma = 0.14$)

$$\text{with } \Delta^{13}C_{pl} = \frac{\delta^{13}C_{atm} - \delta^{13}C_{pl}}{1 + \frac{\delta^{13}C_{pl}}{1000}} \quad (2)$$

First of all, we recalculated the root mean squared error ($\sigma = 0.14$) of the Rey et al. (2013) equation with the dataset of Kohn (2010). In order to calculate leaf discrimination ($\Delta^{13}C_{pl}$), the $\delta^{13}C_{atm}$ values of atmospheric CO_2 previously measured in air bubbles trapped within the Vostok ice cores between 43 and 20 ka are used (Leuenberger et al., 1992; Schmitt et al., 2012). Based on the carbon isotope compositions of earthworm calcite granules, the mean annual precipitation values during the Middle and Upper Pleniglacial (from ca. 55 to 17 ka) was estimated by computing equation (1) with the results compiled in Table 2. We propagated the root mean squared error through our calculations of MAP providing mean, minimum and maximum values (Table 2).

4. Discussion

Mean annual precipitation estimated from the $\delta^{13}C$ values of earthworm calcite granules sampled from Nussloch profile P8 range from 269^{+226}_{-163} mm to 460^{+289}_{-209} mm with a mean value of 367^{+254}_{-183} mm for the tundra gley horizons (Upper Pleniglacial) and 305^{+230}_{-166} mm for the arctic and boreal brown soils (Middle Pleniglacial) (Fig. 3). These values are considered in first approximation to represent mean annual precipitation that could be different from estimates of edaphic humidity.

Throughout the period spanning from 50 to 20 ka, the $\delta^{13}C$ values of loess organic matter in Nussloch have been interpreted as corresponding to 280^{+120}_{-60} to 460^{+80}_{-160} mm with maxima close to 500 mm over the glacial period based on an inverse modelling approach, entitled BIOME 4 (Hatté and Guiot, 2005). Our mean palaeoprecipitation estimates are mostly bracketed by these extreme values of precipitation. Moreover, the comparison between the $\delta^{13}C$ of the organic matter from the profile P4 and our calculated $\delta^{13}C$ of vegetation inferred from those of earthworm calcite granules have comparable mean values for a given horizon (Table 3). Among the five samples coming from tundra gleys of profile P8, the $\delta^{13}C$ values of earthworm granules from the two samples from G1 (unit 21) and G7 (unit 35) record a lower amount of precipitation in comparison to the G2a and G2b horizons. This higher amount of precipitation recorded during G2a and G2b formations is supported by the very high proportions (more than 50%) of the hygrophilous mollusc taxa *Succinella oblonga* and is characterized afterwards by a singular humid episode during which *S. oblonga* predominates in the molluscan fauna with the cold and

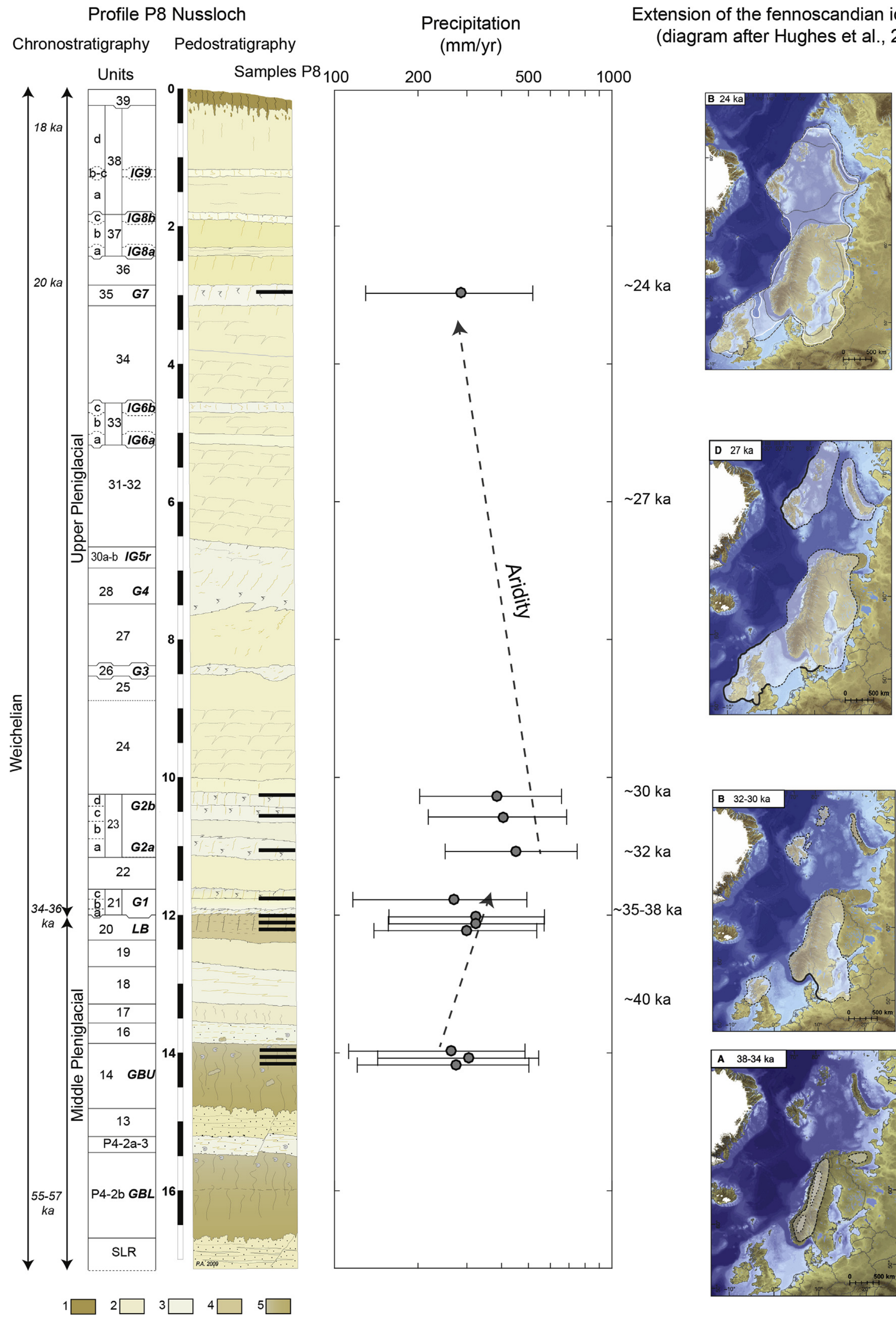

Fig. 3. Stratigraphic sequence of the Nussloch profile P8 with the location of the eleven samples (black bars). The detailed descriptions of the stratigraphy and lithology are available in Antoine et al. (2001, 2009). The detailed chronology of the sequence is available in Moine et al. (2017). 1: Holocene humic topsoil (reworked), 2: loess, 3: tundra gley horizons, 4: arctic brown soil horizon, 5: boreal brown soil horizons. GBL = Lower Gräselberger Boden (boreal brown soil, Bw horizon), GBU = Upper Gräselberger Boden (boreal brown soil, Bw horizon), LB = Lohner Boden (arctic brown soil, Bw horizon), G = major tundra gley (gelic gleysol horizon), IG = incipient tundra gley and r = reworked, ET = Eltviller Tuff. The bars

humid taxa *Columella columella* and with the palustral taxa *Vertigo genesii* (Moine, 2008). In addition, more intense hydromorphic features (stronger reduction, greenish colour, more developed iron oxide precipitation around root tracks) are also clearly observed in units G2a-b (Antoine et al., 2001). The reconstruction of the landscape evolution zone from laminated Eifel maar sediments in Germany recorded four flood events around 30 to 31 ka which likely indicate both intense spring snowmelt as well as summer rain events (Sirocko et al., 2016). A more humid context during G2 formation is also coherent with the laminated facies of the overlying loess unit 24, which suggests a stronger impact of snow melt events (niveo-aeolian) compared to pure homogeneous loess (Antoine et al., 2009). Similar results are inferred from loess sequences located in southeast Germany (Saxony). The stratigraphy of several loess profiles along with the development of tundra gleys horizons reflect warmer and wetter conditions (Meszner et al., 2013).

This period corresponds to the maximal growth phase of the Fennoscandia ice cap from 33 to 27 ka (Hughes et al., 2016), implying increased moisture conditions. The maximum extension of the SW margin of the Scandinavian ice cap is reached between 27 and 19 ka, which implies drier conditions at mid-latitudes. Moreover, though the sediment features do not change and the mollusc abundance (number of individuals) remains minimal throughout the laminated loess unit 24, the strong decrease in richness (number of species) contemporaneous with the maximum in grain size index values characterises a decrease in both vegetation and humidity suggesting the occurrence of a significant change in the atmospheric circulation during a timespan including Heinrich H2 event (Moine et al., 2008). Comparable results are found in eastern loess sequences during the MIS 2. The transport of larger grain sizes indicates a highest wind speed, which implied a high accumulation rate in an arid and cold (development of large ice-wedges) environment (Meszner et al., 2013).

The oxygen isotope compositions of earthworm calcite granules recorded a mean palaeotemperature higher during the formation of boreal and arctic brown soils (12 ± 4 °C) than during the development of tundra gley horizons (10 ± 4 °C) (Prud'homme et al., 2016), whereas the carbon isotope compositions did not record a significance difference between these two pedostratigraphical units (Table 1). However, the pedostratigraphy and the mollusc assemblages highlight both environmental and vegetation changes between the horizon formed during the middle and upper Pleniglacial interstadials (Moine et al., 2008; Antoine et al., 2009). The boreal and arctic brown soils are associated with a high mollusc concentration showing a high proportion of mesophilous species, which lived in an open environment (Moine et al., 2005). Sedimentological data indicate an important weathering leaching of $CaCO_3$ from the profile may lead to an enrichment in clay particles and a densification of the vegetation cover associated with bioturbation processes, high proportions of molluscs and earthworms granules and an increase in organic matter content (Antoine et al., 2001; Hatté et al., 2001; Moine et al., 2008; Prud'homme et al., 2015). The compilation of these data reveals the development of a dense steppe vegetation which can be associated with the presence of large mammal fauna (mammoths, wholly rhinoceros) as observed in the Northern France loess sequences (Antoine et al., 2016). On the contrary, the tundra gley horizons formed during the Upper Pleniglacial are characterized by a lower mollusc content but a high proportion of hygrophilous species (*Succinella Oblonga*; Moine et al., 2008). Moreover, these tundra gley horizons are associated with cryostructures indicating that they were developed in a permafrost environment (Antoine et al., 2009; Jary, 2009; Taylor and Lagroix, 2015). These horizons are formed by hydromorphic processes resulting from the thawing of the active layer (evidence of gelifluction) associated with root development and by a high earthworm calcite granule concentration indicating milder conditions compared to the deposition of typical loess units (Antoine et al., 2009). The vegetation cover is less dense than during the Middle Pleniglacial interstadials, which suggests a vegetation type like a tundra environment as demonstrated by the BIOME 4 climate simulations performed by Hatté and Guiot (2005).

Therefore, the comparison between pedostratigraphy, mollusc assemblage and granule-derived palaeoprecipitation revealed three distinct phases during the Upper Pleniglacial at Nussloch: a phase with relatively humid conditions until 26.5 ka associated with the formation of the thickest tundra gley horizons (G1, G2, G3 et G4), a less humid second phase corresponding to the development of incipient tundra gleys (IG6 and IG5) until ~23/22 ka and a third phase with drier conditions following the formation of the tundra gley G7. These phases may be correlated with the growth dynamics of the Fennoscandia ice cap.

5. Conclusion

Earthworm calcite granule $\delta^{13}C$ values from Nussloch, Rhine Valley, Germany, have been used to estimate the palaeoprecipitation during the development of the Last Glacial tundra

Table 2
Mean annual precipitation with minimum and maximum values (MAP in mm.yr^{-1}) calculated from earthworm calcite granule $\delta^{13}C$ values (Table 1) are given along with local plant $\delta^{13}C$ values estimated using the carbon isotope fractionation factor between organic matter and granule mineralized carbon (Canti, 2009) at Nussloch, Germany (profile P8), for tundra gley horizons (G7, G2a, G2b, G2d, G1) and arctic and boreal brown soils (Lohner Boden (LB) and Gräselberger Boden Upper (GBU)). Atmospheric $\delta^{13}C$ values come from Leuenberger et al. (1992) and Schmitt et al. (2012) and the radiocarbon dates were performed by Moine et al. (2017).

Sample	Date (ka)	Horizon	$\delta^{13}C_{plants}$[a] (‰ V-PDB)	$\delta^{13}C_{atm}$ (‰ V-PDB)	Log_{10}(MAP-300) (±sigma)	$\Delta13C_{pl}$	Mean MAP (mm/yr)	Min MAP (mm/yr)	Max MAP (mm/yr)
P8_1	23.6	G7	−23.7 ± 0.7	−6.49	2.77 ± 0.14	17.6	293	130	518
P8_2	30.1	G2a	−24.3 ± 0.9	−6.43	2.83 ± 0.14	18.3	394	203	658
P8_3	30.2	G2b	−24.4 ± 0.9	−6.43	2.85 ± 0.14	18.4	415	218	687
P8_4	31.1	G2d	−24.9 ± 0.9	−6.60	2.87 ± 0.14	18.7	460	251	749
P8_5	33.5	G1	−24.1 ± 0.8	−7.07	2.75 ± 0.14	17.4	275	116	494
P8_6	35.4	LB	−24.4 ± 0.6	−6.92	2.80 ± 0.14	17.9	331	157	571
P8_7	35.4	LB	−24.3 ± 0.9	−6.92	2.79 ± 0.14	17.8	330	156	569
P8_8	35.4	LB	−24.2 ± 0.8	−6.92	2.77 ± 0.14	17.7	306	139	536
P8_9	45.0	GBU	−23.9 ± 0.8	−6.90	2.75 ± 0.14	17.4	269	112	486
P8_10	45.0	GBU	−24.2 ± 0.8	−6.90	2.78 ± 0.14	17.7	312	143	544
P8_11	45.0	GBU	−23.9 ± 1.2	−6.90	2.75 ± 0.14	17.4	281	121	502

[a] Values are calculated from the $\delta^{13}C$ of granule calcites taking into account the isotopic fractionation factor that takes place during the mineralization of the earthworm diet.

illustrate the standard deviations (2σ) associated with the mean carbon isotope ratios. The rainfall can be correlated with the development of the Fennoscandia ice sheet (Hughes et al., 2016). During the growth of the ice sheet, the environmental conditions were wetter in western Europe whereas during the maximal extension the conditions were drier.

Table 3
Comparison between carbon isotopic values of corrected earthworm granules ($\delta^{13}C_{plants}$) extracted from Nussloch loess profile P8 and the carbon isotopic values of organic matter from profile P4 (C. Hatté pers. comm).

Sample	Horizon	$\delta^{13}C_{plants}$ (‰ V-PDB)	Horizon Depth P4 (cm)	^{13}Com (‰ V-PDB)
P8_1	G7	−23.7 ± 0.7	1450–1455	−23.7 ± 0.1
P8_2	G2a	−24.3 ± 0.9	720–725	−24.3 ± 0.1
P8_3	G2b	−24.4 ± 0.9	680–685	−24.6 ± 0.1
P8_4	G2d	−24.9 ± 0.9	625–630	−25.0 ± 0.1
P8_5	G1	−24.1 ± 0.8	555–560	−24.4 ± 0.1
P8_6	LB	−24.4 ± 0.6	530–535	−24.9 ± 0.1
P8_7	LB	−24.3 ± 0.9	520–525	−24.6 ± 0.1
P8_8	LB	−24.2 ± 0.8	510–515	−24.3 ± 0.2
P8_9	GBU	−23.9 ± 0.8		
P8_10	GBU	−24.2 ± 0.8		
P8_11	GBU	−23.9 ± 1.2		

gley horizons, and arctic brown boreal soils developed in a loessic environment. The carbon isotope compositions of the granules have been corrected from an isotopic fractionation factor that takes place between the carbon ingested by the earthworms and the carbon output in the granules. Taking into account this isotopic fractionation, δ^{13}C values of granules indicate that these palaeosols developed from a C_3-type vegetation during the Last Glacial. This study shows for the first time that the carbon isotope compositions of the earthworm calcite granules can be used to reconstruct the mean annual palaeoprecipitation that was estimated by using an empirical relationship determined between present-day plant leaf isotopic discrimination and the mean annual precipitation. Computed estimates are 367^{+254}_{-183} mm for tundra gley horizons and 305^{+230}_{-166} mm for brown soils. Currently, comparable values are found in the region of the South of Central Russia (close to the Baikal Lake), where the mean annual precipitation is about 260 mm (Oulan Oude) to 480 mm (Irkoutsk). As carbon isotope compositions of earthworm calcite granules reflect the contemporaneous vegetation cover, we propose this isotopic record as a new and valuable proxy to reconstruct Quaternary mean annual amounts of precipitation from the study of loess sequences.

Acknowledgements

This work has received financial supports from the LabEx DynamiTe (ANR-11-LABX-0046), as part of the “Investissements d'Avenir” program, from the ANR-08-BLAN-0227 ‘ACTES’ (DDR) and IUF (CL). The authors thank Magali Seris for her help in the laboratory and Serge Legendre for his help in the statistical treatment of data. The authors thank Dominik Faust and an anonymous reviewer for their helpful comments that helped us to improve the scientific content of this work.

Appendix A. Supplementary data

Supplementary data related to this article can be found at https://doi.org/10.1016/j.quascirev.2017.11.017.

References

Ampel, L., Bigler, C., Wohlfarth, B., Risberg, J., Lotter, A.F., Veres, D., 2010. Modest summer temperature variability during DO cycles in western Europe. Quat. Sci. Rev. 29, 1322–1327.

Antoine, P., Guerin, G., Deschodt, L., Goval, E., Locht, J.-L., Paris, C., et al., 2016. Upper Pleistocene loess-palaeosol records from Northern France in the European context: environmental background and dating of the middle Palaeolithic. Quat. Int. 411, 4–24.

Antoine, P., Rousseau, D.-D., Moine, O., Kunesch, S., Hatté, C., Lang, A., Tissoux, H., Zöller, L., 2009. Rapid and cyclic aeolian deposition during the Last Glacial in European loess: a high-resolution record from Nussloch, Germany. Quat. Sci. Rev. 28, 2955–2973.

Antoine, P., Rousseau, D.-D., Zöller, L., Lang, A., Munaut, A.-V., Hatté, C., Fontugne, M., 2001. High-resolution record of the last interglacial–glacial cycle in the Nussloch loess–palaeosol sequences, Upper Rhine Area, Germany. Quat. Int. 76, 211–229.

Barta, G., 2014. Paleoenvironmental reconstruction based on the morphology and distribution of secondary carbonates of the loess-paleosol sequence at Sütto, Hungary. Quat. Int. 319, 64–75.

Becze-Deak, J., Langohr, R., Verrecchia, E., 1997. Small scale secondary $CaCO_3$ accumulations in selected sections of the European loess belt. Morphological forms and potential for paleoenvironmental reconstruction. Geoderma 76, 221–252.

Bibus, E., Frechen, M., Kösel, M., Rähle, W., 2007. Das jungpleistozäne Löss sprofil von Nuss sloch (SW-Wand) im Aufschluss der Heidelberger Zement AG. Eiszeitalt. Ggw 56, 227–255.

Bond, G., Heinrich, H., Broecker, W., Labeyrie, L., McManus, J., Andrews, J., Huon, S., Jantschik, R., Clasen, S., Simet, C., et al., 1992. Evidence for massive discharges of icebergs into the North Atlantic Ocean during the last glacial period. Lett. Nat. 360.

Bräm, H., 1956. Was sind Arion kinkelini Wenz und A. hochheimensis Wenz. Eclogae Geol. Helv. 49, 593–598.

Briones, M., López, E., Méndez, J., Rodríguez, J., Gago-Duport, L., 2008. Biological control over the formation and storage of amorphous calcium carbonate by earthworms. Mineral. Mag. 72, 227–231.

Canti, M., 2009. Experiments on the origin of d13C in the calcium carbonate granules produced by the earthworm Lumbricus terrestris. Soil Biol. Biochem. 41, 2588–2592.

Canti, M., Bronk-Ramsey, C., Hua, Q., Marshall, P., 2015. Chronometry of pedogenic and stratigraphic events from calcite produced by earthworms. Quat. Geochronol. 28, 96–102.

Canti, M.G., 1998. Origin of calcium carbonate granules found in buried soils and Quaternary deposits. Boreas 27, 275–288.

Canti, M.G., Piearce, T.G., 2003. Morphology and dynamics of calcium carbonate granules produced by different earthworm species: the 7th international symposium on earthworm ecology Cardiff·Wales 2002. Pedobiologia 47, 511–521.

Cerling, T.E., Quade, J., 1993. Stable carbon and oxygen isotopes in soil carbonates. Geophys. Monogr. Ser. 78, 217–231.

Dansgaard, W., Johnsen, S., Clausen, H., Dahl-Jensen, D., Gundestrup, N., Hammer, C., Hvidberg, C., Steffensen, J., Sveinbjörnsdottir, A., Jouzel, J., et al., 1993. Evidence for general instability of past climate from a 250-kyr ice-core record. Nature 364, 218–220.

Darwin, C., 1881. The Formation of Vegetable Mould through the Action of Worms, with Observations on their Habits, 288 pp. John Murray, London.

Diefendorf, A.F., Mueller, K.E., Wing, S.L., Koch, P.L., Freeman, K.H., 2010. Global patterns in leaf 13C discrimination and implications for studies of past and future climate. Proc. Natl. Acad. Sci. 107, 5738–5743.

Freeman, K.H., Mueller, K.E., Diefendorf, A.F., Wing, S.L., Koch, P.L., 2011. Clarifying the influence of water availability and plant types on carbon isotope discrimination by C3 plants. Proc. Natl. Acad. Sci. 108, E59–E60. https://doi.org/10.1073/pnas.1102556108.

Gago-Duport, L., Briones, M., Rodriguez, J., Covelo, B., 2008. Amorphous calcium carbonate biomineralization in the earthworm's calciferous gland: pathways to the formation of crystalline phases. J. Struct. Biol. 162, 422–435.

Genty, D., Combourieu-Nebout, N., Peyron, O., Blamart, D., Wainer, K., Mansuri, F., Ghaleb, B., Isabello, L., Dormoy, I., von Grafenstein, U., et al., 2010. Isotopic characterization of rapid climatic events during OIS3 and OIS4 in Villars Cave stalagmites (SW-France) and correlation with Atlantic and Mediterranean pollen records. Quat. Sci. Rev. 29, 2799–2820.

Gocke, M., Pustovoytov, K., Kühn, P., Wiesenberg, G., Löscher, M., Kuzyakov, Y., 2011. Carbonate rhizoliths in loess and their implications for paleoenvironmental reconstruction revealed by isotopic composition: 13C; 14C. Chem. Geol. 283, 251–260.

Haesaerts, P., Damblon, F., Gerasimenko, N., Spagna, P., Pirson, S., 2016. The Late Pleistocene loess-palaeosol sequence of Middle Belgium. Quat. Int. 411 (Part A), 25–43. https://doi.org/10.1016/j.quaint.2016.02.012. Middle Palaeolithic in North-West Europe: Multidisciplinary Approaches.

Harrison, S., Goñi, M.S., 2010. Global patterns of vegetation response to millennial-scale variability and rapid climate change during the last glacial period. Quat. Sci. Rev. 29, 2957–2980.

Hatté, C., Antoine, P., Fontugne, M., Lang, A., Rousseau, D.-D., Zöller, L., 2001. 13C of Loess organic matter as a potential proxy for paleoprecipitation. Quat. Res. 55, 33–38.

Hatté, C., Gauthier, C., Rousseau, D.-D., Antoine, P., Fuchs, M., Lagroix, F., Marković, S., Moine, O., Sima, A., 2013. Excursions to C4 vegetation recorded in the Upper Pleistocene loess of Surduk (Northern Serbia): an organic isotope geochemistry study. Clim. Past. 9, 1001–1014.

Hatté, C., Guiot, J., 2005. Palaeoprecipitation reconstruction by inverse modelling using the isotopic signal of loess organic matter: application to the Nussloch loess sequence (Rhine Valley, Germany). Clim. Dyn. 25, 315–327.

Heinrich, H., 1988. Origin and consequences of cyclic ice rafting in the northeast Atlantic Ocean during the past 130,000 years. Quat. Res. 29, 142–152.

Hodson, M.E., Benning, L.G., Demarchi, B., Penkman, K.E., Rodriguez-Blanco, J.D., Schofield, P.F., Versteegh, E.A., 2015. Biomineralisation by earthworms–an investigation into the stability and distribution of amorphous calcium carbonate. Geochem. Trans. 16, 1–16.

Hughes, A.L.C., Gyllencreutz, R., Lohne, Ø.S., Mangerud, J., Svendsen, J.I., 2016. The last Eurasian ice sheets – a chronological database and time-slice reconstruction, DATED-1. Boreas 45, 1–45. https://doi.org/10.1111/bor.12142.

Jary, Z., 2009. Periglacial markers within the Late Pleistocene loess–palaeosol sequences in Poland and Western Ukraine. Quat. Int. 198, 124–135.

Koeniger, P., Barta, G., Thiel, C., Bajnóczi, B., Novothny, Á., Horváth, E., Techmer, A., Frechen, M., 2014. Stable isotope composition of bulk and secondary carbonates from the Quaternary loess-paleosol sequence in Sütt\Ho, Hungary. Quat. Int. 319, 38–49.

Kohn, M.J., 2011. Reply to Freeman et al.: carbon isotope discrimination by C3 plants. Proc. Natl. Acad. Sci. 108, E61. https://doi.org/10.1073/pnas.1103222108.

Kohn, M.J., 2010. Carbon isotope compositions of terrestrial C3 plants as indicators of (paleo) ecology and (paleo) climate. Proc. Natl. Acad. Sci. 107, 19691–19695.

Lee, M., Hodson, M., Langworthy, G., 2008. Crystallization of calcite from amorphous calcium carbonate: earthworms show the way. Mineral. Mag. 72, 257–261.

Leuenberger, M., Siegenthaler, U., Langway, C., 1992. Carbon isotope composition of atmospheric CO2 during the last ice age from an Antarctic ice core. Nature 357, 488–490.

Meszner, S., Kreutzer, S., Fuchs, M., Faust, D., 2013. Late Pleistocene landscape dynamics in Saxony, Germany: paleoenvironmental reconstruction using loess-paleosol sequences. Quat. Int. 296, 94–107. https://doi.org/10.1016/j.quaint.2012.12.040. Closing the gap - North Carpathian loess traverse in the Eurasian loess belt 6th Loess Seminar, Wrocław, Poland Dedicated to Prof. Henryk Maruszczak.

Moine, O., 2008. West-European malacofauna from loess deposits of the Weichselian Upper Pleniglacial: compilation and preliminary analysis of the database. Quaternaire 19, 11–29.

Moine, O., Antoine, P., Hatté, C., Landais, A., Mathieu, J., Prud'homme, C., Rousseau, D.-D., 2017. The impact of Last Glacial climate variability in west-European loess revealed by radiocarbon dating of fossil earthworm granules. Proc. Natl. Acad. Sci. 114, 6209–6214. https://doi.org/10.1073/pnas.1614751114.

Moine, O., Rousseau, D.-D., Antoine, P., 2008. The impact of Dansgaard–Oeschger cycles on the loessic environment and malacofauna of Nussloch (Germany) during the Upper Weichselian. Quat. Res. 70, 91–104.

Moine, O., Rousseau, D.D., Antoine, P., 2005. Terrestrial molluscan records of Weichselian Lower to Middle Pleniglacial climatic changes from the Nussloch loess series (Rhine Valley, Germany): the impact of local factors. Boreas 34, 363–380.

Moreno, A., Svensson, A., Brooks, S.J., Connor, S., Engels, S., Fletcher, W., Genty, D., Heiri, O., Labuhn, I., Perşoiu, A., et al., 2014. A compilation of Western European terrestrial records 60–8 ka BP: towards an understanding of latitudinal climatic gradients. Quat. Sci. Rev. 106, 167–185.

NGRIP members, 2004. High-resolution record of Northern Hemisphere climate extending into the last interglacial period. Nature 431, 147–151. https://doi.org/10.1038/nature02805.

O'Leary, M.H., 1981. Carbon isotope fractionation in plants. Phytochemistry 20, 553–567.

Prud'homme, C., Antoine, P., Moine, O., Turpin, E., Huguenard, L., Robert, V., Degeai, J.-P., 2015. Earthworm calcite granules: a new tracker of millennial-timescale environmental changes in Last Glacial loess deposits. J. Quat. Sci. 30, 529–536.

Prud'homme, C., Lécuyer, C., Antoine, P., Moine, O., Hatté, C., Fourel, F., Martineau, F., Rousseau, D.-D., 2016. Palaeotemperature reconstruction during the Last Glacial from d18O of earthworm calcite granules from Nussloch loess sequence. Ger. Earth Planet. Sci. Lett. 442, 13–20.

Rasmussen, S.O., Bigler, M., Blockley, S.P., Blunier, T., Buchardt, S.L., Clausen, H.B., Cvijanovic, I., Dahl-Jensen, D., Johnsen, S.J., Fischer, H., et al., 2014. A stratigraphic framework for abrupt climatic changes during the Last Glacial period based on three synchronized Greenland ice-core records: refining and extending the INTIMATE event stratigraphy. Quat. Sci. Rev. 106, 14–28.

Rey, K., Amiot, R., Lécuyer, C., Koufos, G., Martineau, F., Fourel, F., Kostopoulos, D., Merceron, G., 2013. Late Miocene climatic and environmental variations in northern Greece inferred from stable isotope compositions (δ 18 O, δ 13 C) of equid teeth apatite. Palaeogeogr. Palaeoclimatol. Palaeoecol. 388, 48–57.

Rousseau, D., Antoine, P., Hatté, C., Lang, A., Zöller, L., Fontugne, M., Othman, D.B., Luck, J., Moine, O., Labonne, M., et al., 2002. Abrupt millennial climatic changes from Nussloch (Germany) Upper Weichselian eolian records during the Last Glaciation. Quat. Sci. Rev. 21, 1577–1582.

Rousseau, D.-D., 1991. Climatic transfer function from Quaternary molluscs in European loess deposits. Quat. Res. 36, 195–209.

Rousseau, D.-D., Boers, N., Sima, A., Svensson, A., Bigler, M., Lagroix, F., Taylor, S., Antoine, P., 2017. (MIS3 & 2) millennial oscillations in Greenland dust and Eurasian aeolian records – a paleosol perspective. Quat. Sci. Rev. 169, 99–113. https://doi.org/10.1016/j.quascirev.2017.05.020.

Rousseau, D.-D., Sima, A., Antoine, P., Hatté, C., Lang, A., Zöller, L., 2007. Link between European and North Atlantic abrupt climate changes over the last glaciation. Geophys. Res. Lett. 34, L22713.

Sánchez Goñi, M.F., Landais, A., Fletcher, W.J., Naughton, F., Desprat, S., Duprat, J., 2008. Contrasting impacts of Dansgaard–Oeschger events over a western European latitudinal transect modulated by orbital parameters. Quat. Sci. Rev. 27, 1136–1151.

Schmitt, J., Schneider, R., Elsig, J., Leuenberger, D., Lourantou, A., Chappellaz, J., Köhler, P., Joos, F., Stocker, T.F., Leuenberger, M., et al., 2012. Carbon isotope constraints on the deglacial CO2 rise from ice cores. Science 336, 711–714.

Schönhals, E., Rohdenburg, H., Semmel, A., 1964. Ergebnisse neuerer Untersuchungen zur Würmlöß-Gliederung in Hessen. EG – Quat. Sci. J. 15, 199–206.

Semmel, A., 1973. C. Area between the Scandinavian and the Alpine Glaciation periglacial sediments and their stratigraphy. Eiszeitalt. Ggw 23/24, 293–305.

Sirocko, F., Knapp, H., Dreher, F., Förster, M.W., Albert, J., Brunck, H., Veres, D., Dietrich, S., Zech, M., Hambach, U., Röhner, M., Rudert, S., Schwibus, K., Adams, C., Sigl, P., 2016. The ELSA-Vegetation-Stack: reconstruction of Landscape Evolution Zones (LEZ) from laminated Eifel maar sediments of the last 60,000 years. Glob. Planet. Change 142, 108–135. https://doi.org/10.1016/j.gloplacha.2016.03.005.

Taylor, S.N., Lagroix, F., 2015. Magnetic anisotropy reveals the depositional and postdepositional history of a loess-paleosol sequence at Nussloch (Germany). J. Geophys. Res. Solid Earth 120, 2859–2876.

Tedrow, J.C., 1977. Soils of the Polar Landscapes. Rutgers University Press.

Tissoux, H., Valladas, H., Voinchet, P., Reyss, J., Mercier, N., Falguères, C., Bahain, J.-J., Zöller, L., Antoine, P., 2010. OSL and ESR studies of Aeolian quartz from the Upper Pleistocene loess sequence of Nussloch (Germany). Quat. Geochronol. 5, 131–136.

Versteegh, E.A.A., Black, S., Hodson, M.E., 2017. Carbon isotope fractionation between amorphous calcium carbonate and calcite in earthworm-produced calcium carbonate. Appl. Geochem 78, 351–356. https://doi.org/10.1016/j.apgeochem.2017.01.017.

Zech, M., Tuthorn, M., Detsch, F., Rozanski, K., Zech, R., Zöller, L., Zech, W., Glaser, B., 2013. A 220ka terrestrial δ18O and deuterium excess biomarker record from an eolian permafrost paleosol sequence. NE-Siberia. Chem. Geol. 360, 220–230. https://doi.org/10.1016/j.chemgeo.2013.10.023.